Research article Available online www.ijsrr.org ISSN: 2279–0543

International Journal of Scientific Research and Reviews

Investigation on B-site Titanium doped $La_{0.67}Sr_{0.33}MnO_3$ CMR Manganite by Newly Developed Hybrid Method

G. D. Jadav, P. V. Kanjariya, S. K. Chavda and J. A. Bhalodia*

CMR & HTSC Laboratory, Department of Physics, Saurashtra University, Rajkot – 360 005, Gujarat, India. *Email: jabrajkot@rediffmail.com

ABSTRACT

Since the discovery of the phenomenon of colossal magnetoresistance (CMR) in the $La_{1-x}A_xMnO_3$ (A = Sr, Ca, Ba, etc.) system, there has been extensive research activities on these doped perovskites. The polycrystalline $La_{0.67}Sr_{0.33}Mn_{0.94}Ti_{0.06}O_3$ sample was prepared by a newly developed hybrid method (sol-gel method + solid state reaction method). The XRD confirms that the sample was in single phase (with no detectable secondary phases) having a rhombohedral structure in hexagonal lattice having a space group $R\bar{3}c$. Rietveld refinement was performed using FullProf software for detailed structural investigation. TGA analysis verifies that the precursor shows three step weight loss profiles and does not melt up to the temperature of 1050 °C. A quantitative analysis of the energy dispersive spectroscopy (EDS) data indicates that the observed concentration of elements is very close to the calculated values from its chemical formula. Typical SEM micrograph shows that the sample has fine and clear grain boundaries (GBs). In ρ-T measurement, metal to insulator transition temperature (T_{MI}) was observed at 230 K in absence of external magnetic field. The applied magnetic field suppressed the resistivity peak significantly and the resistivity peak shifts towards higher temperature and MR% also riseswith increment of in magnetic field. The dielectric constant (ε') and dissipation factor (tan δ) were measured at 60, 70, 80, 90 and 100 ˚C in the frequency range of 20 KHz to 1 MHz as a function of temperature. Effect of nonmagnetic isovalent substitution at magnetic Mn site in $La_{0.67}Sr_{0.33}MnO_3$ on structural, CMR and dielectric properties will be discussed in this communication.

KEY WORDS: CMR, XRD, Dielectric

***Corresponding author**

J. A. Bhalodia

CMR & HTSC Laboratory, Department of Physics,

Saurashtra University, Rajkot – 360 005,

Gujarat, India.

Email: jabrajkot@rediffmail.com

INTRODUCTION

A well-known manganite systems with general formula, $A_{1-x}B_xMnO_3$ (A = La, Pr, Nd, Dy, B = Ba, Ca, Sr, Pb) exhibits colossal magnetoresistance (CMR) has attracted renowned interest in experimental and theoretical for a long time [1]. The intrinsic CMR effect in the perovskite manganites, which is caused by the double exchange mechanism (DE), is found on a magneticfield scale of several tesla and a narrow temperature range. The studies have also been motivated by the potential applications of these materials [2].

Hole-doped rare earth manganites show interdependent transport and magnetic properties and are a subject of recent interest due to their remarkable physical properties, like colossal magnetoresistance. The correlation between metallic conduction and ferromagnetism results from Zener double exchange interaction between Mn^{+3} and Mn^{+4} via oxygen 2p orbitals. The nature of magnetic ordering in the entire compositional range depends on the relative concentrations of Mn^{+3} and Mn^{+4} on structural properties, via Mn–O–Mn angles and length. In order to understand the mechanism involved in the DE interaction, many works have been done through doping at A site. Surprisingly, fewer studies have been carried out on the substitution effects at Mn-sites, it does not only introduce lattice distortion, but can also reduce the number of Mn^{+3} or Mn^{+4}, an essential ingredient for the DE interaction [3-11].

In this paper, we report the results of asystematic study of structural, microstructural, electrical and dielectric properties of the compound with composition $La_{0.67}Sr_{0.33}Mn_{0.94}Ti_{0.06}O_3$ (LSMTO). As the non-magnetic Ti^{+4} ion has no 3d electrons, it is expected that the total number of 3d electrons will decrease due to Ti substitution [3].

EXPERIMENTAL

The polycrystalline $La_{0.67}Sr_{0.33}Mn_{0.94}Ti_{0.06}O_3$ compound was prepared by a newly developed hybrid method (sol-gel method + solid-state reaction method) [12-14]. The high purity starting chemicals $La(CH_3CO_2)_3.H_2O$ (Lanthanum Acetate), $Sr(CH_3CO_2)_2$ (Strontium Acetate) and $Mn(CH_3CO_2)_2.4H_2O$ (Manganese Acetate) were taken in stoichiometric ratio. All the three chemicals were dissolved into acetic acid and double distilled water having 1:1 volume ratio.Obtain 0.6 M solution of precursorand continuous stirring is required to achieve a sol state of the material and the precursor solution was dehydrated at 80 ^oC. Further heat treatment at slightly higher temperature ~150 ^oC for 4 hours resulted into the gel form through the gelation process. The gel was dried to obtain the black powder of mixture. High purity TiO_2 (nano powder) was added as per the required

concentration of Ti into mixture of black powder and the whole mixture was ground for 4 hours. The Ti doped black powder was heated at 400 ^{o}C for 6 hours. Further, the heated TiO_2 added black powder was re-heated at 600 ^{o}C for 8 hours to obtain the well calcined black powder. Finally the powder was pressed into pellets under 2 ton pressures for 4 minutes using the hydraulic press. Final product in the form of pellets was sintered at 1300 ^{o}C for 24 hours. Thus, single phase polycrystalline LSMTO sample was prepared.

RESULT AND DISCUSSION

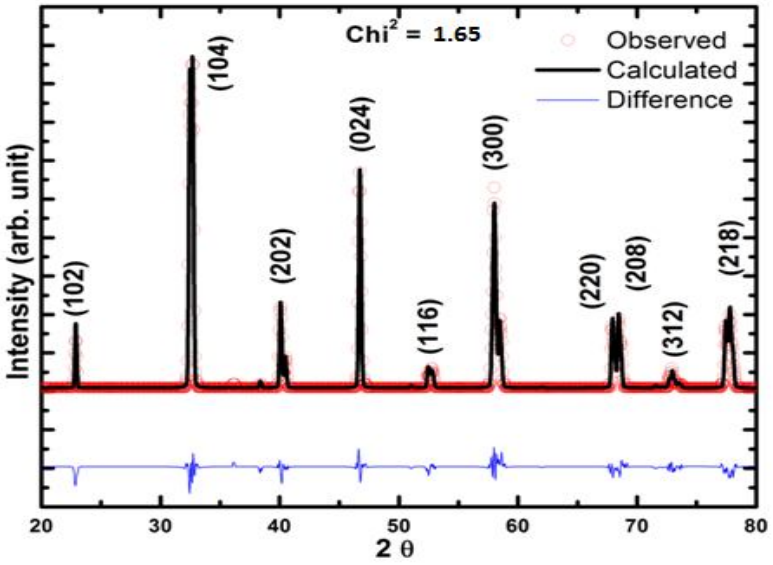

Figure No. 1: "Rietveld refined XRD plot of LSMTO."

Table No. 1: "Rietveld refined obtained values from XRD data for LSMTO."

Sample		**LSMTO**
Unit Cell Parameters	**a & b (A°)**	5.5148
	c (A°)	13.3719
V (A°^{3})		352.18
Space Group		$R\bar{3}c$
Structure		Rhombohedral
FWHM		0.5130
Particle Size (nm)		16.86
X-ray Density (gm/cm^3)		6.35

The phase formation in LSMTO sample was studied by powder X-ray diffractometer (Philips Xpert MPD) with Cu-Kα radiation at room temperature. The sample was scanned in an invariable mode from 20^{o} – 80^{o} with 0.02 degree step size. The Rietveld analysis is a refinement method for powder diffraction pattern to study the crystallographic structure. The refinement of the XRD of the sample was made using FULLPROF program. Figure No. 1 shows Rietveld refinement of XRD graph for LSMTO sample. XRD graph confirms that the sample is in single phase with no detectable secondary phase or phases and the sample has a rhombohedral structure in hexagonal lattice with $R\bar{3}c$ space group. Table No. 1 shows the obtained values of lattice parameters. The available literature on un-doped $La_{0.7}Sr_{0.3}MnO_3$ (LSMO) confirms that the LSMO has a rhombohedral structure [15] in hexagonal lattice with $R\bar{3}c$ space group. So, it is concluded that due to the substitution of Mn^{+4} by Ti^{+4}, the structure does not undergo any transformation.

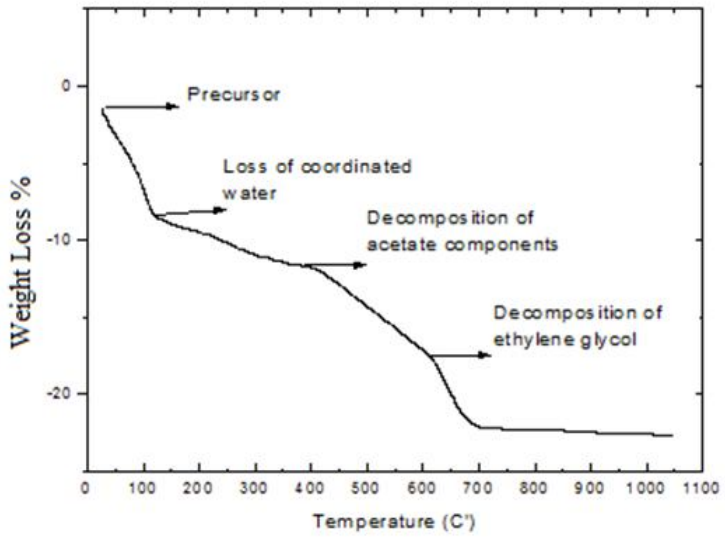

Figure No. 2: "The TGA curve of LSMTO precursor."

The TGA involves measurement of a change in weight of a sample as the temperature is increased at pre determined rate. The weight loss versus temperature plot for the LSMTO precursor (Figure No. 2) could be divided into three stages. The first stage of the TGA profile, with the weight loss of about 8 % to 9 % of its original mass at the temperature range of 40 ºC to 110 ºC is attributed to the loss of water and low boiling organic species. The second stage weight loss (around 11 % to 12 %) in the temperature range of 110 ºC to 400 ºC is attributed to the decomposition of the related coordination species, acetate and oxide components. The third stage of TGA shows a weight loss of about 22 % in the temperature range of 400 ºC to 690 ºC is attributed to the decomposition of ethylene glycol. Above 700 ºC, there is no mass change. It is the stable state of precursor. The precursor has been found not to melt up to the temperature, 1050 °C.

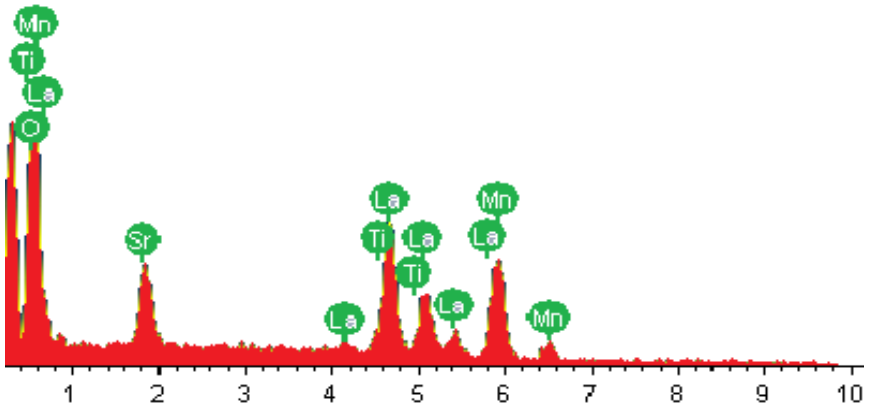

Figure No. 3: "The EDSspectrum of LSMTO."

For verifying the stoichiometric composition in the sample, the energy-dispersive X-ray spectroscopy (EDS) was carried out. Figure No. 3 shows the EDS spectrum for LSMTO sample. Name of each elements, observed and calculated values of Weight % are tabulated in Table No. 2. The observed concentration of each element is very close to its calculated values from its chemical formula. This result of EDS spectrum confirms that, there is no impurity element present in the LSMTO sample.

Table No. 2: "Measured and calculated elemental weight % of LSMTO."

Elements	Measured weight %	Calculated weight %
La	45.53	43.02
Sr	10.05	11.63
Mn	23.06	22.85
Ti	1.87	1.27
O	19.49	21.23
Total	**100**	**100**

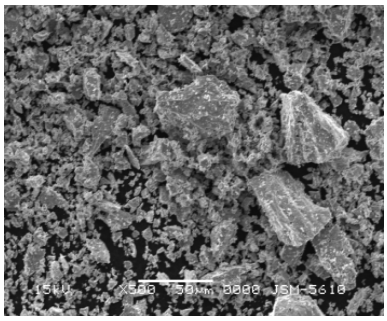

Figure No. 4: "SEM micrograph of LSMTO."

The microstructural measurement (SEM) is essential for understanding the grain growth, grain morphology, shape of the grains and grain size distribution. Figure No. 4 shows the typical SEM micrograph for LSMTO, the sample possesses fine and clear grain boundaries and average grain size of around 1 µm was observed.

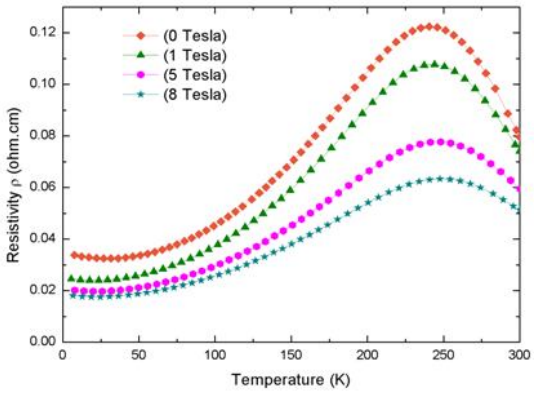

Figure No. 5: "Electrical resistivity as a function of temperature for LSMTO."

The electrical resistivity measurement for LSMTO sample was carried out using standard four probe resistance measurement technique with and without applied magnetic field. Figure No. 5 shows the temperature dependence of resistivity for LSMTO sample measured within a temperature range of 5 K to 300 K without magnetic field and at the external magnetic field of 1 T, 5 T and 8 T. The resistivity graph illustrates that as the magnetic field is increase the resistivity decrease and the metal to insulator transition temperature (T_{MI}) shifts towards the room temperature.

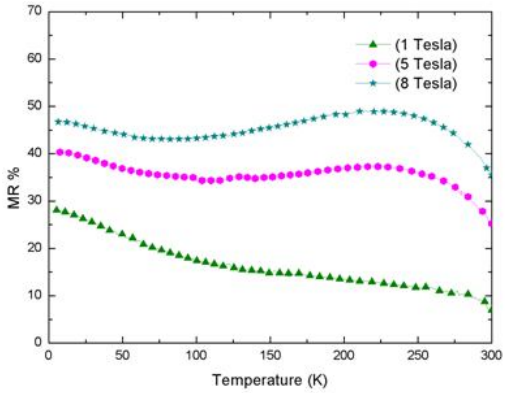

Figure No. 6: "Variation in MR % with temperature and magnetic field for LSMTO."

The LSMTO sample shows the resistivity suppression under applied magnetic field of 1 T, 5 T and 8 T. The temperature dependent magnetoresistance (MR) was calculated within a temperature range of 5 K to 300 K under the magnetic field of 1 T, 5 T and 8 T. Magnetoresistance was calculated using the formula:

$$MR\ \% = [(\rho_o - \rho_H)/\rho_o] \times 100 \qquad \ldots\ldots\ldots\ldots (1)$$

Where, ρ_o and ρ_H represent the resistivity without and applied magnetic field respectively. The maximum room temperature MR (35 %) was observed at 8 T, which is comparatively larger MR than at 1 T and 5 T. This result indicates that the magnetoresistance effect increases with applied magnetic field.

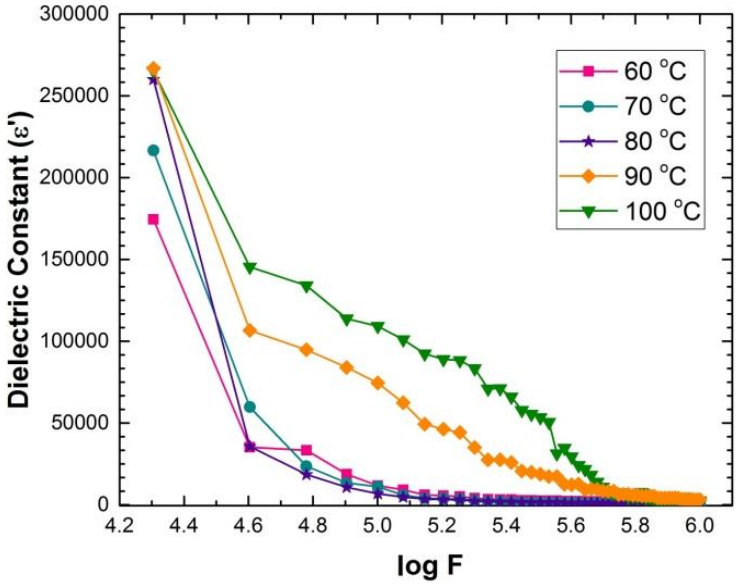

Figure No. 7: "Variation indielectric constant as a function of log F for LSMTO."

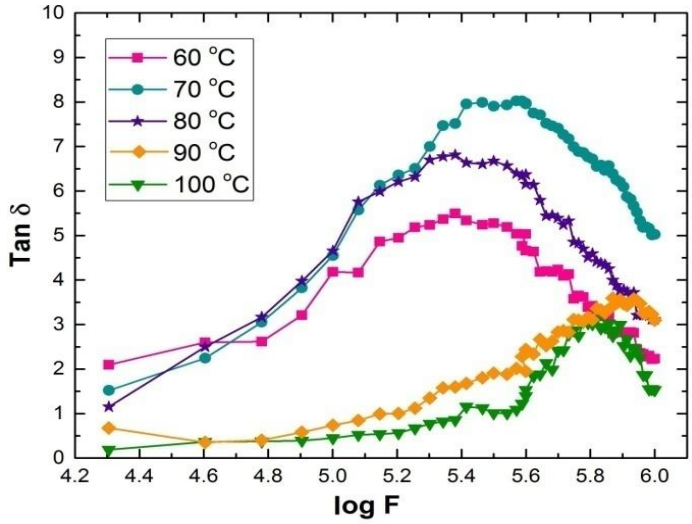

Figure No. 8: "Variation in dielectric loss as a function of log F for LSMTO."

The dielectric constant (ε') and dielectric loss (tan δ) were measured at 60, 70, 80, 90 and 100 ˚C in the frequency range of 20 KHz to 1 MHz.Figure No. 7 shows the dielectric constant vs log F for the LSMTO sample, it can be concluded that for each temperature, as frequency increases the dielectric constant decreases and nearly at 0.6 MHz frequency; dielectric constant reaches at its minimum value and becomes equal for all temperatures. At 20 KHz frequency, dielectric constant increaseswith temperature, from 20 to 40 KHz frequency dielectric constant rapidly decreases at all the temperatures. Above 40 KHz frequency, dielectric constant for 90 and 100 °C decrease slowly compared to other temperature. Highest dielectric constant at low frequency is around 2.7×10^5 for 80, 90 and 100 °C. Figure No. 8 shows that the graph of dielectric loss vs log F, from this graph we observed that the at 20 KHz frequency it is minimum for 100 °C and maximum for 60 °C. As frequency increases the dielectric loss is rapidly increases for 60, 70 and 80 °C. The maximum dielectric loss for 60, 70 and 80 °C is 5.5 (at 0.21 MHz), 8.1 (at 0.40 MHz) and 6.8 (at 0.20 MHz) respectively. For 90 and 100 °C, dielectric loss slowly increases up to 0.40 MHz after that it increases rapidly, the maximum dielectric loss for 90 and 100 °C is 3.6 (at 0.63 MHz) and 3.0 (at 0.87 MHz) respectively.

CONCLUSIONS

To summarize, we have successfully synthesized $La_{0.67}Sr_{0.33}Mn_{0.94}Ti_{0.06}O_3$ sample by a newly developed hybrid method (sol-gel method + solid state reaction method).The XRD pattern confirms that the sample was in single phase having a rhombohedral structure in hexagonal lattice with the space group, $R\bar{3}c$. TGA analysis verifies that the precursor shows three step weight loss profiles and

does not melt up to the temperature of 1050 °C. The EDS data indicate that the observed concentration of each element is very close to the calculated value from its chemical formula. Typical SEM micrograph shows that the sample has fine and clear grain boundaries (GBs). Resistivity measurements illustrates that the applied magnetic field suppresses the resistivity peak significantly and the resistivity peak shifts towards higher temperature. MR% rises with incensement of magnetic field. Dielectric measurement reveals that the maximum dielectric constant is observed at low frequency and highest temperature. At low frequency, dielectric loss increases and reaches to its maximum value subsequently decreases rapidly for all the temperatures at high frequency.

ACKNOWLEDGEMENTS

Authors are thankful to Dr. R. Rawat from UGC-DAE CSR, Indore for resistivity measurements and Prof G. K. Solanki from S. P. University, V. V. Nagar for dielectric measurements.

REFERENCES

[1] C. P. Walter, S. A. Halim, Z. Zalita, Z. A. Talib, Z. A. Hassan, W. M. Daud W. Yusoff and M. Mazni, Structural and physical properties of $La_{0.4}Ba_{0.6}Mn_{0.4}Ti_{0.6-x}Sn_xO_3$ ceramic samples, J. Fiz. Mal., 2007; 28: 109-113.

[2] P. Kameli, The effect of TiO_2 doping on the structure and magnetic and magnetotransport properties of $La_{0.75}Sr_{0.25}MnO_3$ composite, Journal of applied physics, 2005; 98: 043908.

[3] N. Kallel, G. Dezanneau, J. Dhahri, M. Oumezzine and H. Vincent, Structure, magnetic and electrical behaviour of $La_{0.7}Sr_{0.3}Mn_{1-x}Ti_xO_3$ with $0 \leq x \leq 0.3$, Journal of Magnetism and Magnetic Materials, 2003; 261: 56–65.

[4] H. Y. Hwang, S. W. Cheong, P. G. Radaelli, M. Marezio and B. Batlogg, Phys. Rev. Lett., 1995; 75: 914.

[5] K.H. Ahn, X.W. Wu, K. Liu, C.L. Chien, Phys. Rev. B, 1996; 54: 15299.

[6] R.Van. Helmolt, L. Haupt, K. Bahner and U. Sondermann,Solid State Commun., 1992; 82: 693.

[7] L. Righi, P. Gorria, J. Guti!errez and J.M. Barandiaran,J. App. Phys., 1997; 81: 5767.

[8] M. Pissas, G. Kallias, E. Devlin, A. Simopoulos and D.Niarchos, J. Appl. Phys., 1997; 81: 5770.

[9] J. Gutierrez, A. Pena, J.M. Barandiaran, J.L. Pizarro, T. Hernandez, L. Lezama, M. Insausti and T. Rojo, Phys. Rev. B, 2000; 61: 9028.

[10] N. Gayathri, A.K. Raychaudhuri, S.K. Tiwary, R.Gundakaram, A. Arularj and C.N.R. Rao, Phys.Rev. B, 1997; 56: 1345.

[11] B.J. Kennedy, C.J. Howard, G.J. Thorogood, M.A.T.Mestre and J.R. Hester, J. Solid State Chem.,2000; 155: 455.

[12] J. A. Bhalodia, P. V. Kanjariya, S. R. Mankadia, G. D. Jadav, "Structural and Magnetic Characterization of $BiFeO_3$ Nanoparticles Synthesized Using Auto-combustion Technique", Int. J. ChemTech Res. (IJCRGG), 2014; 6(3): 2144.

[13] J. A. Bhalodia, G. D. Jadav, H. D. Shah, S. R. Mankadia, P. V. Kanjariya, "Enhanced Room Temperature Magnetoresistance Property of Co and Ti Doped $La_{0.7}Sr_{0.3}MnO_3$", Int. J. ChemTech Res. (IJCRGG), 2014; 6(3): 2193.

[14] J. A. Bhalodia, S. R. Mankadia, P. V. Kanjariya, H. D. Shah, G. D. Jadav, "Influence of Grain Size on Structure, Electrical Transport and Magnetoresistive Properties of Nanophasic $La_{0.8}Na_{0.2}MnO_3$ Manganite", Int. J. ChemTech Res. (IJCRGG), 2014; 6(3): 2147.

[15] S. R. Mankadia and J. A. Bhalodia, Electrical Transport and Magnetoresistive Properties of Nanophasic $La_{1-X}A_XMnO_3$ (A = Ca, Sr and Na) ManganitesAIP Conf. Proc., 2013; 1536: 947-948.